metals

MDPI

Article

Melt Protection of Mg-Al Based Alloys

María J. Balart *, Jayesh B. Patel * and Zhongyun Fan

BCAST, Brunel University, Uxbridge, Middlesex, UB8 3PH, UK; zhongyun.fan@brunel.ac.uk
* Correspondence: maria.balart@brunel.ac.uk (M.J.B.); jayesh.patel@brunel.ac.uk (J.B.P.); Tel.: +44-1895-267105 (M.J.B. & J.B.P.); Fax: +44-1895-269758 (M.J.B. & J.B.P.)

Academic Editor: Hugo Lopez
Received: 23 March 2016; Accepted: 23 May 2016; Published: 30 May 2016

Abstract: This paper reports the current status of Mg melt protection in view to identify near-future challenges, but also opportunities, for Mg melt protection of Mg-Al based alloys. The goal is to design and manufacture sustainable Mg alloys for resource efficiency, recycling and minimising waste. Among alternative cover gas technologies for Mg melt protection other than SF_6: commercially available technologies containing—HFC-134a, fluorinated ketone and dilute SO_2—and developed technologies containing solid CO_2, BF_3 and SO_2F_2, can potentially produce toxic and/or corrosive by-products. On the other hand, additions of alkaline earth metal oxides to Mg and its alloys have developed a strong comparative advantage in the field of Mg melt protection. The near-future challenges and opportunities for Mg-Al based alloys include optimising and using CO_2 gas as feedstock for both melt protection and grain refinement and TiO_2 additions for melt protection.

Keywords: magnesium alloys; oxidation; high temperature; liquid state; reactive element effect; CO_2 gas

1. Introduction

The design and manufacturer [1] of sustainable Mg alloys and the need to reduce environmental impacts are the main factors that advance the development of new processes such as the replacement of SF_6 gas [2–5]; and industrial furnace design, including lid design, addressing energy efficiency and metal losses in new and existing furnaces. In comparison to structural materials such as Al and steel, Mg components for automotive applications have better greenhouse gas emission performance (GHGEP) based on regular lifecycle assessments. However, this GHGEP advantage of Mg components can be significantly reduced depending on the production technology adopted, *i.e.*, electrolytic *versus* thermal process, in both cases assuming replacement of SF_6 cover gas [6].

Since SF_6 has been identified as a GHG [5,7,8], the protective films formed on molten magnesium and its alloys under gas protection have been an active subject of research, with the aim of finding suitable industrial alternatives to SF_6 gas for melt protection [7–21]. The use of SF_6 gas will be banned from the European Union from 2018 [22] (as cited in Reference [23]), in which case, replacement of SF_6 as a cover gas in the Mg industry would no longer be eligible as Clean Development Mechanism (CDM) project or Joint Implementation (JI) project, nor sell the reduced emission as 'carbon credits' [24]. The International Magnesium Association (IMA) has recognised the need to identify melt protection alternatives with both low toxicity and GHG emissions [25,26]. In this paper, taking as a starting point a brief overview of the work on Mg melt protection, the near-future challenges, but also opportunities, for melt protection of Mg-Al based alloys are identified.

2. Reactive Element Effect

It has been seventy-nine years since the 'rare earth element effect' was first proposed [27]. The original premise was that it was possible to obtain Ni-20Cr alloys in order to improve resistance to

high temperature oxidation by additions of rare earth elements. A few years later the original concept of rare earth element effect was adapted and extended to other elements with high affinity to oxygen, to increase the corrosion resistance of refractory alloys without impairing their creep resistance. At this time, the 'active elements' suggested by Pfeil's patent were Sc, Y, La, Ti, Zr, Hf, Nb, Ta, Al, Si, Ce, Pr, Nd, Pm, Sm, Eu, Gd, Tb, Dy, Ho, Er, Tm, Yb, Lu and Th [28] (as cited in Reference [29]). The topic became more commonly known as the 'Reactive Element Effect' (REE). A detailed review of the REE on high temperature oxidation of Mg was recently published by Czerwinski [27], including Ca, Be, Sr and Ti, which readily oxidise when exposed to oxygen, give the magnesium alloy improved resistance to oxidation during melting. The high affinity to oxygen of those and all other rare earth elements are the basis of the REE [30–32]. Some examples of Ca, Be, Sr and Ti additions to molten Mg are given below. An Ellingham diagram [33,34] for their oxides including Al and Mg oxides is depicted in Figure 1, from which it can be seen that their affinity to oxygen until ~1000 K (726.85 °C) decreases in the following order Ca > Be > Mg > Sr > Al > Ti.

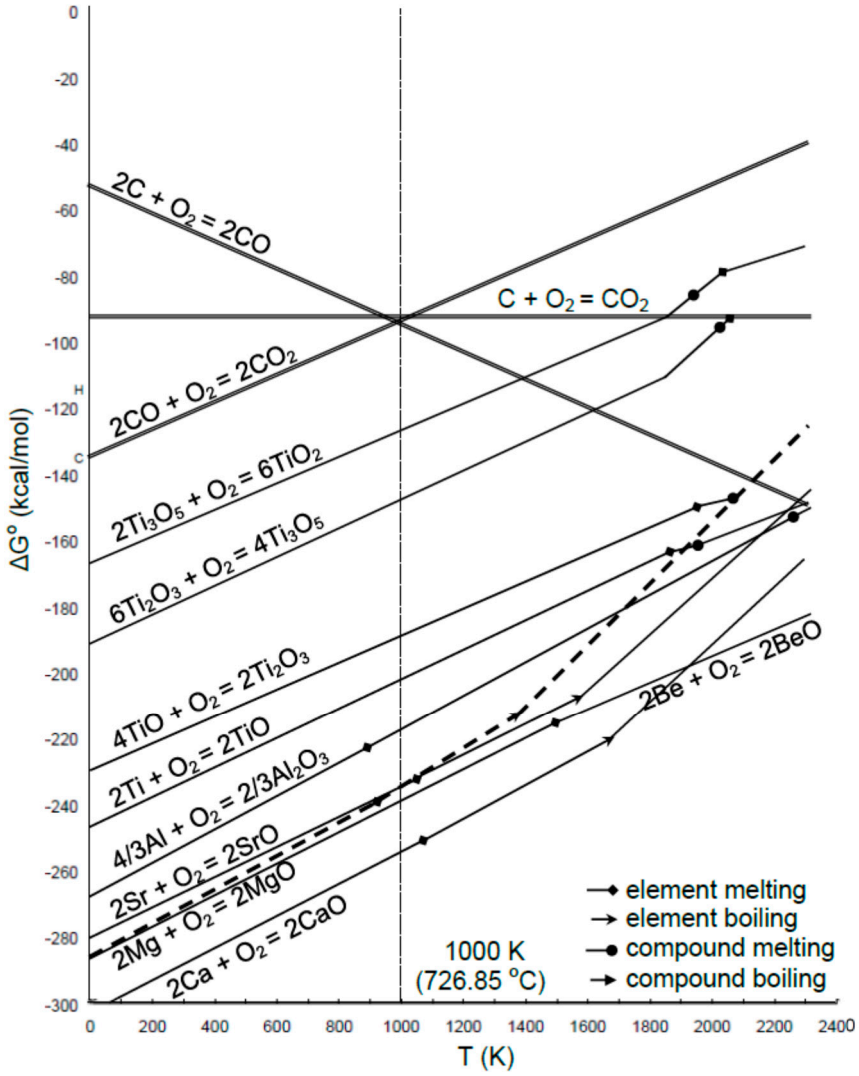

Figure 1. Schematic of the Ellingham diagram for selected oxides [33,34]. Mg oxidation is marked with a dashed line. Adapted from [34], copyright (2006), reprinted with permission of Stanley M. Howard.

2.1. Ca Additions

Sakamoto *et al.* [35] reported that the thin oxide layer formed on the surface of molten Mg—1.5Ca alloy was protective and consisted of an outer layer of CaO and an inner layer composed of a mixture

of CaO and MgO. In a subsequent study by Wiese *et al.* [23] at higher additions of Ca, it was found that the thin oxide layer formed on the surface of molten Mg—7.2%CaO alloy was also protective after exposure at 720 °C for 5 min in both air and SF_6/Ar and by using SEM and TEM techniques, identified the formation of Mg/Mg_2Ca eutectic phase at the inner surface layer and of a mixture of MgO/CaO at the outer surface layer, but also Mg/Mg_2Ca eutectic phase at the outer surface layer, suggesting that Mg_2Ca phase was protective. It is interesting to note that Mg_2F was not found at the surface layer despite using an SF_6/Ar gas mixture in the latter case. This was attributed to be due to the possible protective character of the MgO/CaO mixture, preventing the reaction of SF_6 gas at the surface of the Mg melt.

In practice, additions of CaO to Mg and Mg-Al based alloys can lead to the formation of Mg_2Ca according to reactions (1) and (2), respectively [4]. Note the solubility of Ca in liquid Mg. According to the Mg-rich region of the equilibrium phase diagram of eutectic type for the Mg-Ca system [36], the invariant point is 10.5 at.% Ca at 516.5 °C. Therefore, the presence of Mg_2Ca phase is to be expected for example at 700 °C in high Ca-containing Mg alloys only.

$$10Mg_{(l)} + 4CaO_{(s)} = 4Mg_2Ca_{(s)} + [O_2 + 2MgO\,(\text{dross})] \quad (1)$$

$$\begin{gathered} Mg\,[Al,\ \text{other alloying elements}]_{(l)} + CaO_{(s)} = Mg_2Ca_{(s)} + Al_2Ca_{(s)} + \\ [(Mg,\ Al, \text{other alloying elements})_2Ca_{(s)}] + [O_2 + MgO\,(\text{dross})] \end{gathered} \quad (2)$$

Indeed, recent work by Wiese *et al.* [37,38] confirms the reaction of CaO and the formation of Mg_2Ca laves phase in the bulk of Mg-16Ca + 6CaO and Mg-10CaO (in wt.%) by *in situ* synchrotron measurements of the reaction between molten Mg and CaO. Mg_2Ca and Al_2Ca are Laves phases with crystal structures and melting points of: hexagonal, 714 °C (Mg_2Ca) and cubic, 1079 °C (Al_2Ca), respectively [39]. The additions of alkaline earth metal oxides to Mg and its alloys have developed a strong comparative advantage in the field of Mg melt protection.

2.2. Be Additions

Be has a higher affinity to oxygen than Mg. Trace additions of beryllium in the range between 5 and 30 ppm are made to Mg alloys [40], in particular AZ91D, AM60, AM50 and AZ31 Mg alloys may contain 5–10 ppm Be [27].

2.3. Sr Additions

Rare or alkaline earth metals additions are commonly made to Mg-Al based alloys for creep-resistance applications, e.g., Mg-Al-RE and Mg-Al-Sr alloys [41]. The presence of SrO/MgO in AJ62 alloy would be initially expected according to reaction (3) [42]. Note the solubility of Sr in liquid Mg. At high concentrations of Sr, it could react with molten Mg to form intermetallics such as $Mg_{17}Sr_2$, $Mg_{38}Sr_9$, $Mg_{23}Sr_6$ and Mg_2Sr phases [43], but also SrO could react according to reaction (4) [4].

$$2Mg_{(l)} + 2Sr_{(l)} + 4/3Al_2O_{3(s)} = 2MgO_{(s)} + 2SrO_{(s)} + 8/3Al \quad (3)$$

at 690 °C, $\Delta G^\circ_3 = -947{,}620$ J/mol.

$$\begin{gathered} Mg\,[Al,\ \text{other alloying elements}]_{(l)} + SrO_{(s)} = Mg_2Sr_{(s)} + Al_2Sr_{(s)} + \\ [(Mg,\ Al,\ \text{other alloying elements})_2Sr_{(s)}] + [O_2 + MgO\,(\text{dross})] \end{gathered} \quad (4)$$

From previous studies [42,44], Sr-bearing AJ62 alloy held at 690 for 10 s exhibited higher resistance to oxidation than that of Sr-free AZ91D alloy held at 650 for 10 s, as shown from macroscopic observations of the reaction products formed on the surface in Figure 2, from which it can be seen two distinctive regions of non-nodular growth (in a layer manner) and of nodular growth, indicating two different stages of the surface reaction. Samples from these regions are outlined by the white squares marked 1—non-nodular growth—and 2—nodular growth—in Figure 2. FEG-SEM revealed that all the

morphologies, *i.e.*, sponge-like, nodular and layer, were porous and hence non-protective with respect to the evaporation and oxidation of Mg, Zn and Sr from the corresponding surface of the AZ91D and AJ62 alloy melt, as shown in Figure 3. XRD results from the surface of AZ91D, AZ31, AM60 and AJ61 alloys indicated that, in all these regions, MgO was the main oxidation product along with traces of AlN. Additionally, traces of ZnO reflected the Zn levels of the Mg magnesium alloys and the oxidation conditions investigated.

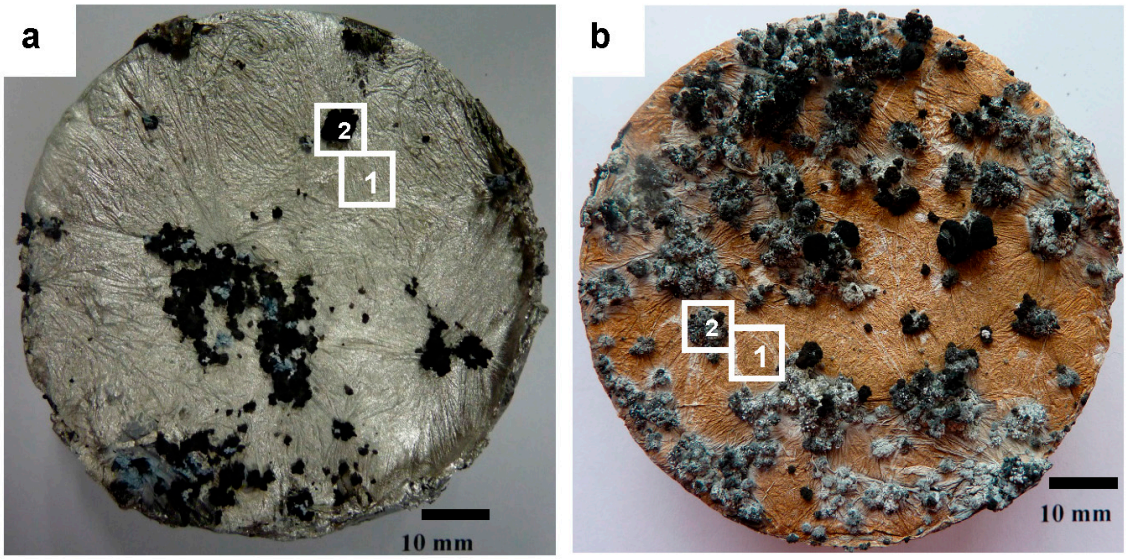

Figure 2. Macroscopic view of surface of Mg alloys exposed to air under two oxidation conditions: (**a**) AJ62 alloy held at 690 °C for 10 s, reprinted with permission from Reference [42], copyright 2014, Taylor & Francis Ltd., www.tandfonline.com; (**b**) AZ91D alloy held at 650 °C for 10 s, reprinted with permission from Reference [44], copyright 2014, Taylor & Francis Ltd., www.tandfonline.com. Marked regions indicate following reaction stages: (1) non-nodular growth in layer manner and (2) nodular growth. AJ62 alloy exhibited higher resistance to high temperature oxidation than that of AZ91D alloy.

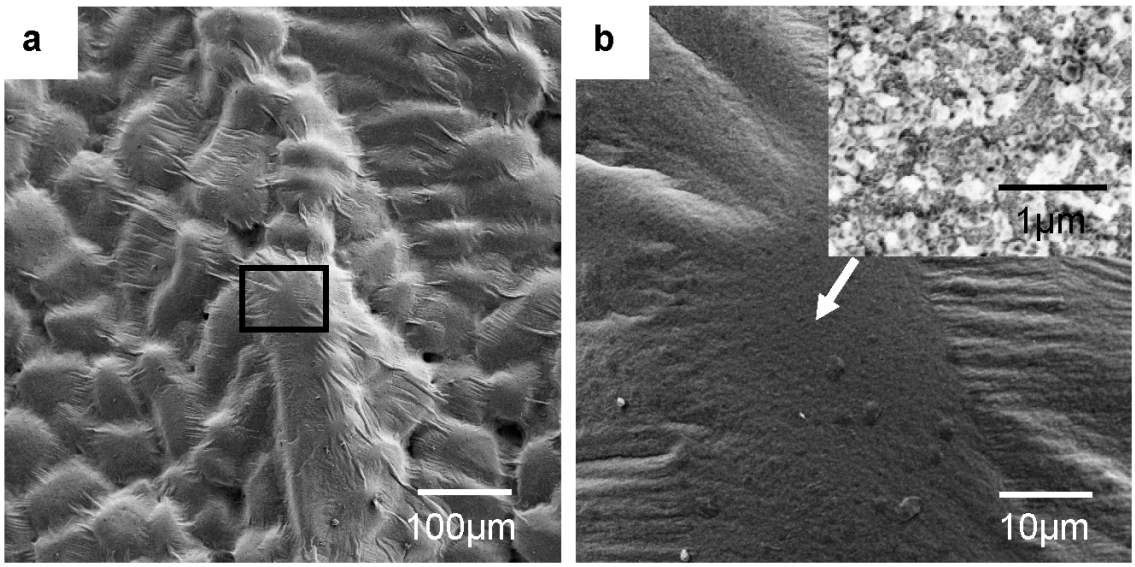

Figure 3. Secondary electron images from region marked 1 (macroscopic non-nodular growth) in Figure 2b, from surface of AZ91D alloy held at 650 °C for 10 s [44] showing (**a**) oxide layer; (**b**) magnification of region outlined by black rectangle in (**a**); detail of predominantly granular MgO nanoparticles (inset).

2.4. Ti Additions

Some notable successes in Mg and Mg-9Al alloy have been an increase of over 30% in strength and elongation with the introduction of O interstitial atoms, 50% increase in formability, double creep resistance and a 10-fold increase in corrosion resistance [45].

First TiO_2 nano-particles having high chemical potential energy are introduced into the Mg melt, and then they decompose to O, Ti and TiO. Subsequently, Ti and TiO having high specific gravity sink down to the bottom of the crucible. Finally, oxygen atoms in the Mg melt will remain interstitial after solidification. This was due to an increase in the activation energy for the formation of MgO.

Ti has been found to inhibit Mg corrosion in aqueous solutions [27], and might also impact greatly on the field of high temperature oxidation of Mg alloys. TiO_2 particles could react at the surface of Mg-Al based alloys. Thermodynamic analysis in conjunction with experimental evidence showed that the formation of TiAl can be favoured at the expense of other Ti_xAl_y compounds [46]. This is because Mg has a higher affinity to oxygen than Ti and Ti reacts preferentially with Al to form TiAl (reaction (7)). TiAl has a high oxidation limit of 900 °C and a low density of 4.1–4.7 gr/cm^3 [46,47]. In contrast, the oxidation resistance of Al_3Ti is much better than those of TiAl and Ti_3Al [47].

$$3TiO_{2(s)} + 7Al_{(l)} = 2Al_2O_{3(s)} + 3TiAl \quad (5)$$

at 700 °C, $\Delta G^\circ_5 = -648{,}733$ J/mol [46]

$$3Mg_{(l)} + Al_2O_{3(s)} = 3MgO_{(s)} + 2Al_{(l)} \quad (6)$$

$\Delta G^\circ_6 = -145{,}810 + 26.32T$ [48], where ΔG° is in J/mol and T is in K.

Reactions (5) and (6) can be combined to obtain the standard Gibbs energy change of reaction (7) at 700 °C.

$$3TiO_{2(s)} + 3Al_{(l)} + 6Mg_{(l)} = 6MgO_{(s)} + 3TiAl_{(s)} \quad (7)$$

$\Delta G^\circ_7 = \Delta G^\circ_5 + 2\Delta G^\circ_6$. At 700 °C, $\Delta G^\circ_7 = -889{,}126$ J/mol, hence, reaction (7) is shifted to the right to form MgO and TiAl.

3. Flux Additions

Typical salt fluxes are chloride KCl, NaCl and $MgCl_2$ and fluoride CaF_2. $MgCl_2$ can be used in Mg alloys containing Al, Zn and Mn alloying elements such as AZ91D, AM60, AM50 and AZ31 representing the majority of commercial Mg alloys. Flux entrapment, release of corrosive gas and melt losses are the major causes for the shift from flux to gas protective atmospheres [49].

4. Alternatives to SF_6 for Mg Melt Protection

Fruehling, investigated protective atmospheres for molten magnesium [50]. Mirak *et al.* [16] summarised the significant findings on protective gases in stagnant melts held isothermally under a mixture of a protective gas (e.g., SF_6, SO_2 or 1,1,1,2-tetrafluoroethane (HFC-134a)) and a carrier gas (e.g., dry air or N_2), based on characterisation of the reaction layer formed on the melt surface by the use of various techniques, including SEM, TEM, X-ray diffraction (XRD), X-ray photoelectron spectroscopy (XPS) and thermogravimetric analysis (TGA) and assessment of the corresponding oxidation behaviour. Mg melt protection in the context of the nature, origin and control of inclusions with regard to reactions with air, fluxes and protective gases during melt treatment, casting and alloying was later reviewed by Lun *et al.* [49].

Melt protection alternatives to both flux-based and SF_6, consisting of active gases: fluorine-based blended gas (HFC-134a), fluorinated ketones (FK) and dilute SO_2 (1.5%) mixed with a carrier gas, generally N_2, CO_2 or dry air, are commercially available [20,25,26]. The work of Ha and Kim [18] showed that hydrofluorocarbon CF_3CH_2F (HFC-134a) possessed better protection properties than do SF_6 and SO_2, using air as a carrier gas. However, since HF can form in a mixture of HFC-134a/air and

is highly corrosive, it was recommended the use of N_2 or CO_2 carrier gases instead of air. The reaction products between Mg melt and SF_6, HFC-134a and FK are MgO and MgF_2. Mg melt can react with SO_2 to form $MgSO_4$, MgO or MgS [49].

On the other hand, several alternative melt protection technologies that are not currently commercialized or readily available have been developed [20,25,26]. Those alternative techniques generate solid CO_2, a small amount of BF_3 gas and SO_2F_2 gas for Mg melt protection. The use of solid CO_2 can generate toxic CO [51]. BF_3 is not a GHG, however, is highly toxic, expensive and require the use of special storage conditions [49]. It should be noted that nowadays the use of SO_2 gas for Mg melt protection might require a SO_2 scrubber system (*i.e.*, flue gas desulfurization (FGD) technology to comply with the environmental legislation) as well as additional costs associated with corrosion of equipment handling dilute SO_2. On the other hand, the Global Warming Potential (100 years) and atmospheric lifetime (years) values are 23,900, 3200 (SF_6); 1300, 14.6 (HFC-134a); ~1, 0.014 (Novec™ 612) and ~1,—(SO_2F_2) compared with the value of 1, 100–150 for CO_2, respectively [25]. As concerns about global climate change grow, search for alternatives exist to reduce GHG emissions including HFCs.

Aarstad [9] tested a mixture of 1% SF_6 in air, N_2, Ar and CO_2 and 1% SO_2 in air, N_2 and CO_2 to determine whether a protective effect was also achieved with other carried gases than air. It was found that when using inert gases N_2 and Ar as carrier gases, no protective film was formed on the surface of the Mg melt. Furthermore, SF_6 in CO_2 was not a successful combination, conversely when air was added to a mixture of SF_6 and CO_2, a protective film was formed on the melt surface. This is because air is necessary for the development of a protective film on the surface of the Mg melt [9]. In a parallel effort, the authors determined the solubility of fluorine in molten Mg in the range between 700 °C and 950 °C [52] and found that it did not appear to be sufficient for direct dissolution of fluorine into the melt to be an alternative to SF_6.

Small amounts of spinel phase can form on the surface oxide layer of molten AZ91 alloy after exposure to air [53] and two plausible mechanisms for its formation were suggested by the authors. The first mechanism [53] was based on a kinetic study of the surface oxidation of liquid Al—3%Mg and Al—3%Mg—3%Si alloys by Salas *et al.* [54], who proposed that oxidation of Mg to MgO reaction (8), can directly expose MgO to subsurface melt regions enriched in Al, depleted in Mg compared to the bulk of the melt. This coupled with the exothermic reaction (8) at a rate sufficient to cause local superheating of the melt may result in the formation of Al_2O_3 and $MgAl_2O_4$ through the endothermic reactions (6) (shifted to the left) and (9), respectively. Spinel would hence form at the alloy/MgO interface.

$$Mg_{(g)} + 1/2O_{2(g)} = MgO_{(s)} \quad (8)$$

$\Delta G^\circ_{MgO} = -612{,}955 + 128.08T$ [14,15,19]

$$4MgO_{(s)} + 2Al_{(l)} = MgAl_2O_{4(s)} + 3Mg_{(l)} \quad (9)$$

$\Delta G^\circ_7 = 110{,}210 - 28.41T$ [48], where ΔG° is in J/mol and T is in K.

The second mechanism [53] was based on an immediate oxidation to Al_2O_3 and MgO and their solid state reaction [55–57] (reaction (10)) to form spinel through-thickness.

$$MgO_{(s)} + Al_2O_{3(s)} = MgAl_2O_{4(s)} \quad (10)$$

at 800 °C, $\Delta G^\circ_{MgAl2O4} = -46{,}700$ J/mol [58].

Recent work is also indicating that there may be approaches to Mg alloy process routes without protective gas other than SF_6 gas. Mg alloy melting can be carried out lowering the oxygen content inside the enclosed area [3] to prevent catastrophic oxidation, ignition and burning of the melt [35,59]. Kim *et al.* [2] demonstrated successfully the development of AZ31 Mg alloy wrought process route without protective gas, instead, by the addition of 0.42 wt.% CaO to AZ31 alloy melt being protected

by N_2 gas in the temperature range from 640 °C to 660 °C. This reveals alternative approaches to Mg melting and demonstrates the need for further research into the entire topic.

Elimination [60] or reduction [61] of protective SF_6 gas has been achieved in the development of innovative processes such as semi-solid injection moulding. However, just as important to process considerations are the addition of inoculants such as MgO [62] and Al_4C_3 [63,64] to produce a grain-refined microstructure. AZ91D chips were mixed with carbon black using a semi-solid injection moulding technique at 630 °C, the *in situ* reaction between aluminium and carbon occurred to form Al_4C_3 particles [64]. The authors found an optimal carbon black addition of 0.23 wt.% to produce a grain-refined microstructure giving improved properties. Carbon's reaction kinetics are critical to the conversion efficiency, which in turn can affect the effectiveness of corrosion resistance.

Pure CO_2 [50] and mixtures up to 20 vol.% air/CO_2 can protect molten magnesium [9,65,66]. Equally important, however, are carbon's reaction kinetics. A thermodynamic analysis by Aarstad [9] predicted that traces of CO (1.0×10^{-7} moles) and O_2 (5.1×10^{-8} moles) were the decomposition products of 1 mole of CO_2 at 700 °C and 1 bar pressure, and that MgO and C were the reaction products between CO_2 and molten Mg. In parallel, Shih *et al.* [67,68] reported the possible reactions that can occur between Mg and, O_2, CO_2 and CO (reactions (8), (11)–(13)). A diagram of the standard Gibbs energy change *versus* temperature for the reactions (11)–(13) is given in Reference [67], from which it can be seen that, reactions (9)–(11) can proceed spontaniously until about 3725 °C, 2475 °C and 1975 °C, respectively. In particular, at 720 °C, $\Delta G^{\circ}_{12} = -592{,}700$ J/mol [66].

$$Mg_{(g)} + CO_{2(g)} = MgO_{(s)} + CO_{(g)} \quad (11)$$

$$Mg_{(l),\ (g)} + 1/2CO_{2(g)} = MgO_{(s)} + 1/2C_{(s)} \quad (12)$$

$$Mg_{(l),\ (g)} + CO_{(g)} = MgO_{(s)} + C_{(s)} \quad (13)$$

Thermo-oxidative experiments of pure Mg in the liquid state [65,66] have been performed by isothermal TGA in pure CO_2 and mixtures up to 20 vol.% air/CO_2 to monitor the surface oxidation kinetics at high temperatures (670 °C, 720 °C and 770 °C) and to relate those to their morphological and structural characteristics at different oxidation stages (2, 3 and 7 min) as determined by SEM. The TGA and SEM results by Emami and Sohn [65,66] indicated that the surface had a double-layer structure. The external layer consisted of non-protective MgO, whereas the internal layer was dense and protective, and composed of a mixture of MgO/C.

Note the solubility of C in liquid Mg. According to the Mg-C equilibrium phase diagram which was proposed in Reference [69], the value of the solubility of C in Mg is approximately 10 at ppm (5 wt. ppm) at 700 °C. The solubility of C in liquid Mg increases with increasing temperature up to 1093.6 °C at 1 bar pressure. All of these results suggest that both melt protection and grain refinement should be considered in developing practical applications for using CO_2 in Mg-Al based alloys.

5. Conclusions

This paper has examined the topic of Mg melt protection. Among alternative cover gas technologies for Mg melt protection other than SF_6: Commercially available technologies containing—HFC-134a, fluorinated ketone and dilute SO_2—and developed technologies containing solid CO_2, BF_3 and SO_2F_2, can potentially produce toxic and/or corrosive by-products. Additions of alkaline earth metal oxides to Mg and its alloys have developed a strong comparative advantage in the field of Mg melt protection.

The near-future challenges and opportunities for Mg-Al based alloys include, optimising and using CO_2 gas as feedstock for both melt protection and grain refinement, and TiO_2 additions for melt protection, in order to design and manufacture sustainable Mg alloys for resource efficiency, recycling and minimising waste.

Acknowledgments: The financial support of Engineering and Physical Sciences Research Council (EPSRC) is gratefully acknowledged.

Author Contributions: All the authors contributed equally to this work.

Conflicts of Interest: The authors declare no conflict of interest.

References and Notes

1. Emley, E.F. *Principles of Magnesium Technology*; Pergamon Press: Oxford, UK, 1966.
2. Kim, S.K.; Lee, J.K.; Yoon, Y.O.; Jo, H.H. Development of AZ31 Mg alloy wrought process route without protective gas. *J. Mater. Process. Technol.* **2007**, *187–188*, 757–760. [CrossRef]
3. Foerster, G. HiLoN: A new approach to magnesium die casting. *Adv. Mater. Process.* **1998**, *154*, 79.
4. Kim, S.K.; Hoseo, J. Magnesium-Based Alloy with Superior Fluidity and Hot-Tearing Resistance and Manufacturing Method Thereof. US Patent 20110236249 A1, 29 September 2011.
5. Dervos, C.T.; Vassiliou, P. Sulfur hexafluoride (SF_6): Global environmental effects and toxic byproduct formation. *J. Air Waste Manag. Assoc.* **2000**, *50*, 137–141. [CrossRef] [PubMed]
6. Aghion, E.; Gurion, B.; Bartos, S.C. Comparative Review of Primary Magnesium Production Technologies as Related to Global climate Change. In Proceedings of the 65th Annual World Magnesium Conference, Warsaw, Poland, 18–20 May 2008; Available online: http://www.citysat.com.pl/~{}omen/2008_World_Mg_Conference_Papers (accessed on 17 January 2016).
7. Cashion, S.P.; Ricketts, N.J.; Hayes, P.C. Characterisation of protective surface films formed on molten magnesium protected by air/SF_6 atmospheres. *J. Light Metals* **2002**, *2*, 37–42. [CrossRef]
8. Cashion, S.P.; Ricketts, N.J.; Hayes, P.C. The mechanism of protection of molten magnesium by cover gas mixtures containing sulphur hexafluoride. *J. Light Metals* **2002**, *2*, 43–47. [CrossRef]
9. Aarstad, K. Protective Films on Molten Magnesium. Ph.D. Thesis, Norwegian University of Science and Technology, Norway, May 2004. Available online: http://www.diva-portal.org/smash/get/diva2:126206/FULLTEXT01.pdf (accessed on 19 March 2016).
10. Aarstad, K.; Tranell, G.; Engh, T.A. Various Techniques to Study the Surface of Magnesium Protected by SF_6. *Magnes. Technol.* **2003**, 5–10. Available online: http://www.academia.edu/24051179/Various_techniques_to_study_the_surface_of_magnesium_protected_by_SF6 (accessed on 26 May 2016).
11. Xiong, S.M.; Liu, X.L. Microstructure, composition, and depth analysis of surface films formed on molten AZ91D alloy under protection of SF_6 mixtures. *Metall. Mater. Trans. A: Phys. Metall. Mater. Sci.* **2007**, *38A*, 428–434. [CrossRef]
12. Wang, X.F.; Xiong, S.M. Oxidation behavior of molten magnesium in atmospheres containing SO_2. *Corros. Sci.* **2011**, *53*, 4050–4057. [CrossRef]
13. Pettersen, G.; Øvrelid, E.; Tranell, G.; Fenstad, J.; Gjestland, H. Characterisation of the surface films formed on molten magnesium in different protective atmospheres. *Mater. Sci. Eng. A* **2002**, *332*, 285–294. [CrossRef]
14. Liu, J.R.; Chen, H.K.; Zhao, L.; Huang, W.D. Oxidation behaviour of molten magnesium and AZ91D magnesium alloy in 1,1,1,2-tetrafluoroethane/air atmospheres. *Corros. Sci.* **2009**, *51*, 129–134. [CrossRef]
15. Chen, H.; Liu, J.; Huang, W. The protective surface film formed on molten ZK60 magnesium alloy in 1,1,1,2-tetrafluoroethane/air atmospheres. *Corros. Sci.* **2010**, *52*, 3639–3645. [CrossRef]
16. Mirak, A.; Davidson, C.J.; Taylor, J.A. Characterisation of fresh surface oxidation films formed on pure molten magnesium in different atmospheres. *Corros. Sci.* **2010**, *52*, 1992–2000. [CrossRef]
17. Chen, H. Effect of melt temperature on the oxidation behaviour of AZ91D magnesium alloy in 1,1,1,2-tetrafluoroethane/air atmospheres. *Mater. Charact.* **2010**, *61*, 894–898. [CrossRef]
18. Ha, W.; Kim, Y.J. Effects of cover gases on melt protection of Mg alloys. *J. Alloy. Compd.* **2006**, *422*, 208–213. [CrossRef]
19. Zhao, L.; Liu, J.R.; Chen, H.K.; Huang, W.D. The characterization of surface films formed on molten magnesium and AZ91D alloy in air/1,1,1,2-tetrafluoroethane atmospheres. *J. Alloy. Compd.* **2009**, *480*, 711–716. [CrossRef]
20. Milbrath, D.S. Development of 3M^{TM}Novec^{TM} 612 Magnesium Protection Fluid as a Substitute for SF_6 over Molten Magnesium. In Proceedings of the 2nd International Conference on SF_6 and the Environment, San Diego, CA, USA, 22 November 2002; Available online: https://www.epa.gov/sites/production/files/2016-02/documents/conf02_milbrath_paper.pdf (accessed on 20 May 2016).

21. Emami, S.; Sohn, H.Y.; Kim, H.G. Formation and evaluation of protective layer over magnesium melt under SF_6/Air atmospheres. *Metall. Mater. Trans. B* **2014**, *45*, 1370–1379. [CrossRef]
22. Regulation (EU) No 517/2014 of the European Parliament and of the Council of 16 April 2014 of fluorinated greenhouse gases and repealing.
23. Wiese, B.; Mendis, C.L.; Ovri, H.; Reichel, H.-P.; Lorenz, U.; Kainer, K.U.; Hort, N. Role of CaO and Cover Gases on Protecting the Cast Surface of Mg. In Proceedings of the 10th International Conference on Magnesium Alloys and Their Applications, Jeju, Korea, 11–16 October 2015; pp. 814–819.
24. Dishon, A. Financial Benefits from SF_6 Emission Reductions. In Proceedings of the 65th Annual World Magnesium Conference, Warsaw, Poland, 18–20 May 2008; Available online: http://www.citysat.com.pl/~{}omen/2008_World_Mg_Conference_Papers (accessed on 17 January 2016).
25. Alternatives to SF_6 for Magnesium Melt Protection. Available online: https://www.epa.gov/sites/production/files/2016-02/documents/magbrochure_english.pdf (accessed on 20 May 2016).
26. Hillis, J.E. The International Program to Identify Alternatives to SF_6 for Magnesium Melt Protection. In Proceedings of the International Conference on SF_6 and the Environment: Emission Reduction Strategies, San Diego, CA, USA, 21–22 November 2002; Available online: https://www.epa.gov/sites/production/files/2016-02/documents/conf02_hillis_paper.pdf (accessed on 20 May 2016).
27. Czerwinski, F. The reactive element effect on high-temperature oxidation of magnesium. *Int. Mater. Rev.* **2015**, *60*, 264–296. [CrossRef]
28. Pfeil, L.B. Improvements relating to hear-resisting alloys containing chromium. UK Patent No. 574088, 20 December 1945.
29. Beranger, G.; Armanet, F.; Lambertin, M. Active Elements in Oxidation and Their Properties. In The Role of Active Elements in the Oxidation Behaviour of High Temperature Metals and Alloys, Proceedings of the European Colloquium Organised by: Commission of the European Communities, Directorate General: Science, Research and Development, Petten, The Netherlands, 12–13 December 1988; Lang, E., Ed.; Elsevier Applied Science: London, UK; New York, NY, USA, 1988; pp. 33–51.
30. Czerwinski, F. Oxidation characteristics of magnesium alloys. *JOM* **2012**, *64*, 1477–1483. [CrossRef]
31. Aydin, D.S.; Bayindir, Z.; Hoseini, M.; Pekguleryuz, M.O. The high temperature oxidation and ignition behaviour of Mg-Nd alloys part I: The oxidation of dilute alloys. *J. Alloy. Compd.* **2013**, *569*, 35–44. [CrossRef]
32. Pint, B.A. Experimental observations in support of the dynamic-segregation theory to explain the reactive-element effect. *Oxid. Metals* **1996**, *45*, 1–37. [CrossRef]
33. Ellingham, H.J.T. Reducibility of oxides and sulfides in metallurgical processes. *J. Soc. Chem. Ind. (Lond.)* **1944**, *63*, 125–133.
34. Howard, S.M. Ellingham Diagrams, Internet Resource for MET 320—Metallurgical Thermodynamics, South Dakota School of Mines and Technology, Rapid City, SD, USA. Available online: http://showard.sdsmt.edu/MET320/Handouts/EllinghamDiagrams/Ellingham_v22_Macro.pdf (accessed on 12 May 2016).
35. Sakamoto, M.; Akiyama, S.; Ogi, K. Suppression of ignition and burning of molten Mg alloys by Ca bearing stable film. *J. Mater. Sci. Lett.* **1997**, *16*, 1048–1050. [CrossRef]
36. Nayeb-Hashemi, A.A.; Clark, J.B. The Ca-Mg (Calcium-Magnesium) system. *Bull. Alloy Phase Diagr.* **1987**, *8*, 58–65. [CrossRef]
37. Wiese, B.; Mendis, C.L.; Tolnai, D.; Stark, A.; Schell, N.; Reichel, H.-P.; Brückner, R.; Kainer, K.U.; Hort, N. CaO dissolution during melting and solidification of a Mg–10 wt.% CaO alloy detected with *in situ* synchrotron radiation diffraction. *J. Alloy. Compd.* **2015**, *618*, 64–66. [CrossRef]
38. Wiese, B.; Tolnai, D.; Mendis, C.L.; Eckerlebe, H.; Hort, N. *In situ* Diffraction of the Melting and the Solidification of Magnesium Alloys Containing CaO. Available online: http://photon-science.desy.de/annual_report/files/2013/20132901.pdf (accessed on 14 January 2016).
39. Pekguleryuz, M.O. Alloying behaviour of magnesium and alloy design. In *Fundamentals of Magnesium Alloy Metallurgy*; Pekguleryuz, M.O., Kainer, K.U., Kaya, A.A., Eds.; Woodhead Publishing Ltd.: Oxford, UK; Cambridge, PA, USA; New Delhi, India, 2003; p. 169.
40. Friedrich, H.E.; Mordike, B.L. *Magnesium Technology: Metallurgy, Design Data, Applications*; Springer-Verlag: Berlin, Germany, 2006; p. 119.
41. Czerwinski, F.; Zielinska-Lipiec, A. The microstructure evolution during semisolid molding of a creep-resistant Mg-5Al-2Sr alloy. *Acta Mater.* **2005**, *53*, 3433–3444. [CrossRef]

42. Balart, M.J.; Fan, Z. Surface oxidation of molten AZ31, AM60B and AJ62 magnesium alloys in air. *Int. J. Cast Metals Res.* **2014**, *27*, 301–311. [CrossRef]
43. Nayeb-Hashemi, A.A.; Clark, J.B. The Mg-Sr (Magnesium-Strontium) system. *Bull. Alloy Phase Diagr.* **1986**, *7*, 149–156. [CrossRef]
44. Balart, M.J.; Fan, Z. Surface oxidation of molten AZ91D magnesium alloy in air. *Int. J. Cast Metals Res.* **2014**, *27*, 167–175. [CrossRef]
45. Kang, H.; Kang, S.; Park, S.; Bae, D. An Interstitial Magnesium Alloy Containing Oxygen Atoms. In Proceedings of the 10th International Conference on Magnesium Alloys and Their Applications, Jeju, Korea, 11–16 October 2015.
46. Payyapilly, J.J. Formation and Growth Mechanisms of a High Temperature Interfacial Layer Between Al and TiO_2. Ph.D. Thesis, Virginia Polytechnic Institute and State University, Blacksburg, VA, USA, 19 November 2008. pp. 77, 79. Available online: https://vtechworks.lib.vt.edu/bitstream/handle/10919/29733/Jairaj.pdf (accessed on 19 March 2016).
47. Umakoshi, Y.; Yamaguchi, M.; Sakagami, T.; Yamane, T. Oxidation resistance of intermetallic compounds Al_3Ti and TiAl. *J. Mater. Sci.* **1989**, *24*, 1599–1603. [CrossRef]
48. Huang, Z.; Sirong, Y. Microstructure characterization on the formation of *in situ* Mg_2Si and MgO reinforcements in AZ91D/Flyash composites. *J. Alloy. Compd.* **2011**, *509*, 311–315. [CrossRef]
49. Lun Sin, S.; Elsayed, A.; Ravindran, C. Inclusions in magnesium and its alloys: A review. *Int. Mater. Rev.* **2013**, *58*, 419–436. [CrossRef]
50. Fruehling, J.W. Protective Atmospheres for Molten Magnesium. Ph.D. Thesis, The University of Michigan, Ann Arbor, MI, USA, 1970.
51. Norbert, H.; Wiese, B.; Dieringa, H.; Ulrich Kainer, K. Magnesium melt protection. *Mater. Sci. Forum* **2015**, *828–829*, 78–81.
52. Aarstad, K.; Syvertsen, M.; Engh, T.A. Solubility of Fluorine in Molten Magnesium. *Magnes. Technol.* **2002**. [CrossRef]
53. Shih, T.S.; Liu, J.B.; Wei, P.S. Oxide films on magnesium and magnesium alloys. *Mater. Chem. Phys.* **2007**, *104*, 497–504. [CrossRef]
54. Salas, O.; Ni, H.; Jayaram, V.; Vlach, K.C.; Levi, C.G.; Mehrabian, R. Nucleation and growth of Al_2O_3/metal composites by oxidation of aluminium alloys. *J. Mater. Res.* **1991**, *6*, 1964–1981. [CrossRef]
55. Wagner, C. Mechanism of counterdiffusion through reaction in the solid state. *Z. Anorg. Allg. Chem.* **1938**, *236*, 320–338. [CrossRef]
56. Carter, R.E. Mechanism of solid state reaction between MgO and Al_2O_3 and MgO and Fe_2O_3. *J. Am. Ceram. Soc.* **1961**, *44*, 116–120. [CrossRef]
57. Hesse, D.; Senz, S. Interfacial reaction mechanisms and the structure of moving heterophase boundaries during pyrochlore- and spinel-forming solid state reactions. *Z. Metallkunde* **2004**, *95*, 252–257. [CrossRef]
58. Gaskell, D.R. Reaction equilibria in systems containing components in condensed solution. In *Introduction to the Thermodynamics of Materials*, 5th ed.; Taylor & Francis Group: New York, NY, USA; London, UK, 2012; p. 430. Available online: https://books.google.co.uk/books?id=3xfcBQAAQBAJ&pg=PA430&lpg=PA430&dq=free+energy+MgAl2O4&source=bl&ots=wGdalbSfqk&sig=bpZG2u3G_ElsbBet6uJOnfBP-oY&hl=en&sa=X&ved=0ahUKEwibgLqn5L3MAhULKx4KHWUKA-kQ6AEIKzAE#v=onepage&q=free%20energy%20MgAl2O4&f=false (accessed on 5 May 2016).
59. Jafari, H.; Idris, M.H.; Ourdjini, A. High temperature oxidation of AZ91D magnesium alloy granule during *in situ* melting. *Corros. Sci.* **2011**, *53*, 655–663. [CrossRef]
60. Czerwinski, F. The oxidation behaviour of an AZ91D magnesium alloy at high temperatures. *Acta Mater.* **2002**, *50*, 2639–2654. [CrossRef]
61. Fan, Z.; Ji, S.; Fang, X.; Liu, G.; Patel, J.B.; Das, A. Development of Rheo-diecasting (RDC) Process for Production of High Integrity Components. In Proceedings of the Shape Casting: 2nd International Symposium, Orlando, FL, USA, 1 May 2007; Crepeau, P.N., Tiryakioglu, M., Campbell, J., Eds.;
62. Wang, Y.; Fan, Z.; Thompson, G. Characterization of magnesium oxide and its interface with alpha Mg in Mg-Al based alloys. *Philos. Mag. Lett.* **2011**, *91*, 516–529. [CrossRef]
63. Lee, Y.C.; Dahle, A.K.; StJohn, D.H. The role of solute in grain refinement of magnesium. *Metall. Mater. Trans. A* **2013**, *31A*, 2895–2906. [CrossRef]

64. Fukuta, T.; Obunai, K.; Ozaki, K.; Shibata, K. Improvement of mechanical properties of injection molded AZ91D alloy by mixing carbon black as a grain refinement additive. In Proceedings of the 10th International Conference on Magnesium Alloys and Their Applications, Jeju, Korea, 11–16 October 2015; pp. 551–557.
65. Emami, S. Formation and Evaluation of Protective Layer Over Magnesium Melt Under Various Gaseous Atmospheres. Ph.D. Thesis, The University of Utah, Salt Lake City, UT, USA, December 2013. Available online: http://content.lib.utah.edu/utils/getfile/collection/etd3/id/2640/filename/2637.pdf (accessed on 19 March 2016).
66. Emami, S.; Sohn, H.Y. Formation and evaluation of protective layer over magnesium melt under CO_2/air mixtures. *Metall. Mater. Trans. B* **2015**, *46*, 226–234. [CrossRef]
67. Shih, T.S.; Chung, C.B.; Chong, K.Z. Combustion of AZ61A under different gases. *Mater. Chem. Phys.* **2002**, *74*, 66–73. [CrossRef]
68. Shih, T.S.; Wang, J.H.; Chong, K.Z. Combustion of magnesium alloys in air. *Mater. Chem. Phys.* **2004**, *85*, 302–309. [CrossRef]
69. Chen, H.L.; Schmid-Fetzer, R. The Mg-C phase equilibria and their thermodynamic basis. *Int. J. Mater. Res.* **2012**, *103*, 1294–1301. [CrossRef]